# Integrated FDTD and Solid-State Device Simulation

Paolo Ciampolini, Luca Roselli, and Giovanni Stopponi

*Abstract*— **A mixed-mode circuit simulation technique is presented, based on the lumped-element finite-difference time-domain (FDTD) scheme. The algorithm is extended to incorporate numerical models of lumped devices. This makes the formulation and characterization of analytical, closed-form models for circuit devices unnecessary and allows for directly correlating device behavior and fabrication process parameters. The code is therefore especially suited for high-speed and microwave IC optimization.**

## I. Introduction

THE finite-difference time-domain (FDTD) algorithm [1], [2] provides a powerful and flexible approach to the numerical solution of Maxwell's equations. Transient regimes can be accurately investigated, accounting for field propagation over almost arbitrary domains. This makes FDTD particularly appealing for the analysis of high-speed and microwave electronic circuits.

Extensions of the FDTD scheme accounting for active, nonlinear elements have been devised [3] based on the coupling of Maxwell's equations with device equations. For basic lumped elements, device equations consist of straightforward $I(V,t)$ relationships, whereas more complex elements are taken into account by assembling equivalent networks of basic bipoles. The formulation of analytical, closed-form device models, however, is not necessarily a trivial task, especially when dealing with integrated [and, most notably, microwave and millimter-wave integrated circuit (MMIC)] technologies. Optimization of IC performance, in fact, involves a large number of fabrication process details; this makes the parameter characterization, as well as the definition of the model itself, quite critical.

A much closer link between the circuit behavior and the fabrication technology can be established by replacing analytical device models with numerical, distributed ones ("device-level" simulation). Following this approach, the device response is directly extracted from its physical and geometrical description, with no need for either formulating specific "device equations" or extracting model parameters.

In this letter, the lumped-element (LE) FDTD scheme is extended to incorporate a numerical device solver, allowing for integrating full-wave analysis of signal propagation and physically accurate device simulation. A somewhat similar approach has been discussed in the work of Thomas *et al.* [4], where a general-purpose device simulator has been interfaced to an FDTD solver. In the present work, instead, an *ad hoc* simulation code has been developed. By connecting the algorithms at a deeper level, a simpler and more efficient interfacing scheme is obtained and tailoring of specific physical models is made possible. Moreover, in this case, both analytical and "distributed" lumped device models can coexist, thus providing a higher degree of flexibility.

Manuscript received June 27, 1996.

The authors are with the Istituto di Elettronica, Università di Perugia, I-06131 Perugia, Italy.

Publisher Item Identifier S 1051-8207(96)07884-1.

## II. The Simulation Technique

In principle, the physical description of a circuit including active semiconductor devices can be obtained from the solution of Maxwell's equations coupled with semiconductor transport equations over the whole domain of interest. Such a comprehensive approach, however, turns out to be computationally prohibitive for most practical circuits. A convenient way of partitioning the analysis domain into simplified subdomains can be found by assuming: 1) ohmic charge transport at the interconnections; and 2) quasistatic regimes for active device. The latter assumption (largely justified, for typical device sizes, up to frequencies of some tens of THz) allows devices to be considered as "lumped" elements with respect to the electromagnetic simulation (EMS), regardless of device simulation (DS) being performed over a distributed domain. Circuit interconnections can therefore be analyzed by solving the Maxwell's equations

$$\nabla \times \vec{H} = \epsilon \frac{d\vec{E}}{dt} + \vec{J}_c \tag{1}$$

$$\nabla \times \vec{E} = -\mu \frac{d\vec{H}}{dt}. \tag{2}$$

The FDTD discretization scheme is used to this purpose, adopting, in this case, a three-dimensional (3-D) Cartesian grid. Interaction with active devices is accounted for by a scheme similar to that illustrated in [5]. In particular, the conduction current density $\vec{J}_c$ in (1) is obtained by summing up two contributions

$$\vec{J}_c = \vec{J}_{cd} + \vec{J}_{cl} \tag{3}$$

where $\vec{J}_{cd} = \sigma \vec{E}$ accounts for the current flowing along the distributed medium and $\vec{J}_{cl}$ includes contributions of lumped elements. Within the latter term, both analytical and numerical device models can be considered. Details about the incorporation of analytical device models into the code have been reported elsewhere [5]; here, the contribution coming from numerical device models will be discussed, based on the numerical solution of a quasistatic semiconductor transport model. The quasistatic approximation allows one to correlate the electrostatic potential $\varphi$ and the charge density through Poisson's equation

$$\nabla \cdot (-\epsilon_s \nabla \varphi) = q(p - n + N) \tag{4}$$

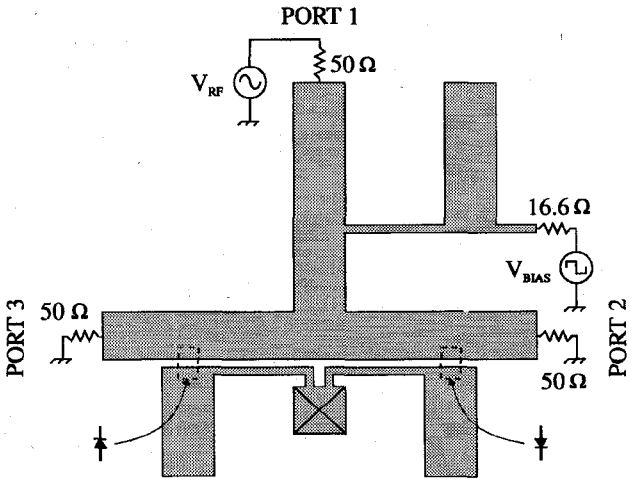


Fig. 1. Sketch of the SPDT structure.

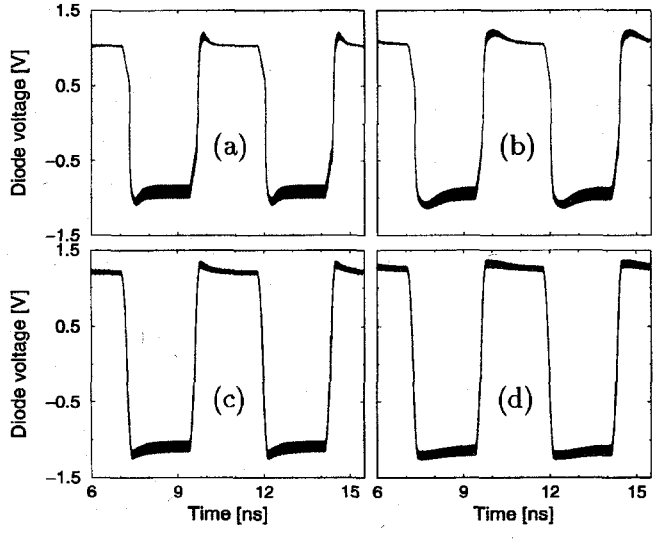


Fig. 2. Time-domain response of the SPDT.

where $N = N_D^+ - N_A^-$ accounts for the net ionized impurity concentrations. Charge conservation for electrons and holes is described by the continuity equations

$$\frac{\partial n}{\partial t} - \frac{1}{q}\nabla \cdot \vec{J}_n = \frac{\partial p}{\partial t} + \frac{1}{q}\nabla \cdot \vec{J}_p = -U \tag{5}$$

whereas current densities for either carrier are expressed through the "drift-diffusion" approximation

$$\vec{J}_n = q\mu_n\left[-n\nabla\varphi + \frac{k_B T}{q}\nabla n\right] \tag{6}$$

$$\vec{J}_p = q\mu_p\left[-p\nabla\varphi - \frac{k_B T}{q}\nabla p\right]. \tag{7}$$

Solution of (4)–(7) provides the time and space distribution of the unknown functions $\varphi, n, p, \vec{J}_n$ and $\vec{J}_p$ within each device. To accomplish the numerical integration, (4) and (5) are discretized over the spatial domain by means of the FD method; in the present implementation, a one-dimensional (1-D) discretization grid is adopted that is independent of the 3-D FDTD mesh. Current densities over such discretized intervals are obtained from (6) and (7) by means of the Scharfetter-Gummel integration scheme [6]. Finally, time-domain integration of (5) is accomplished by the backward-Euler algorithm.

The interface between DS and EMS is obtained by formulating proper boundary conditions. Let us refer, for the sake of simplicity, to a two-terminal device, lumped at the $(i, j, k)$ FDTD cell and oriented along the $x$-direction. Voltage drop across the lumped device is obtained (at $(n+1)$th time step) by integrating the E-field across the $x$-side of the insertion cell (standard Yee's notation [1])

$$\Delta V^{n+1} = -E^{n+1}_{x,(i+\frac{1}{2},j,k)}\Delta x. \tag{8}$$

Assuming an arbitrary reference, and accounting for contact voltage drops (see, e.g., Eq. (8), [7]), provides potential b.c. for DS. The additional unknown $E_x^{n+1}$ is thus introduced into the system (4)–(7), closing the feedback loop between DS and EMS. The related additional equation is found by discretizing and projecting (1) along $x$ direction

$$-\left[\frac{H^{n+(1/2)}_{z,\left(i+\frac{1}{2},j+\frac{1}{2},k\right)} - H^{n+(1/2)}_{z,\left(i+\frac{1}{2},j-\frac{1}{2},k\right)}}{\Delta y} - \frac{H^{n+(1/2)}_{y,\left(i+\frac{1}{2},j,k+\frac{1}{2}\right)} - H^{n+(1/2)}_{y,\left(i+\frac{1}{2},j,k-\frac{1}{2}\right)}}{\Delta z}\right] + \epsilon\frac{E^{n+1}_{x,\left(i+\frac{1}{2},j,k\right)} - E^{n}_{x,\left(i+\frac{1}{2},j,k\right)}}{\Delta t} + J^{n+(1/2)}_{cd,x,\left(i+\frac{1}{2},j,k\right)} + \frac{\left(J^{n+1}_{cl,x,\left(i+\frac{1}{2},j,k\right)} + J^{n}_{cl,x,\left(i+\frac{1}{2},j,k\right)}\right)}{2} = 0. \tag{9}$$

Here, $J_{cl,x}$ represents the lumped-element current contribution, expressed by (6) and (7), and is averaged between time steps $n$ and $n+1$ in order to preserve the "leapfrog" solution scheme typical of FDTD algorithm.

## III. An Application Example

A simulation example is introduced in Fig. 1. It consists of the analysis of a single pole, double throw (SPDT) switch, realized with a Si-MMIC microstrip technology. The sinusoidal RF signal $V_{\mathrm{RF}}$ (ampl. 0.2 V, freq. 76 GHz) is injected at one end of the structure and then forwarded along either output branches, depending on the bias supplied by the square-wave generator $V_{\mathrm{BIAS}}$ (ampl. 2.5 V, freq. 214 MHz). Microstrip stubs and matched loads complete the structure. To isolate the inactive branch, p-i-n diodes have been used, due to their high impedance in the off-state and their compatibility with the high-resistivity silicon, planar process. Feasibility of such Si-MMIC's, suitable for operating frequencies up to 100 GHz,

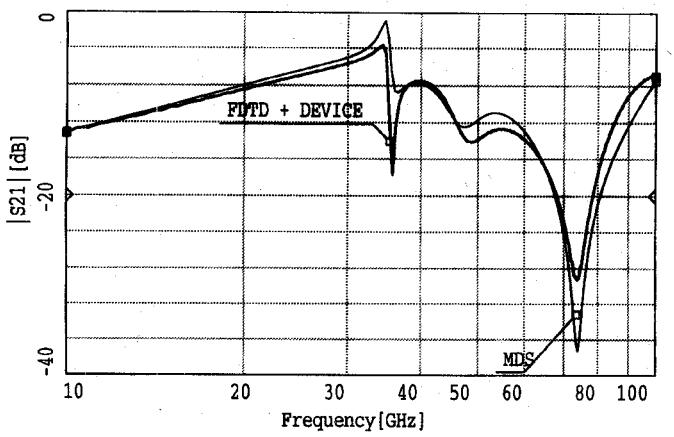


(a)

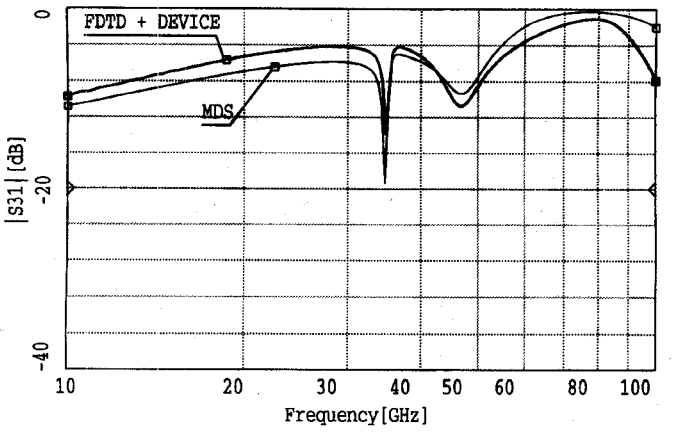


(b)

Fig. 3. (a) Simulated isolation and (b) insertion loss.

has been demonstrated [8]. The formulation of large-signal, analytical models of p-i-n diodes, however, is still a tricky task [9], [10].

Within the present scheme, instead, each diode is directly described by its actual geometry and doping profile. Load resistors, as well as matched voltage sources, are still described by analytical models.

The discretized structure counts $13 \times 79 \times 64$ FDTD cells, while each p-i-n diode is described by a 121-point mesh. The FDTD mesh has been terminated by adopting conventional first order Mur's absorbing boundary conditions [11].

Simulations have been performed to evaluate the influence of some process parameters on the circuit response. Fig. 2 shows transient responses obtained for different doping profiles. The voltage across one of the clamping diodes is shown, depending on both the extrinsic region impurity concentration [$N_D = N_A = 5 \times 10^{18}$ cm$^{-3}$ [(a), (b)], $5 \times 10^{16}$ cm$^{-3}$ [(c), (d)] and the intrinsic layer width ($W = 1.5$ $\mu$m [(a), (c)], 2.5 $\mu$m [(b), (d)]). The frequency behavior of the switch is illustrated in Fig. 3. The bias line, in this case, has been brought to a steady, positive value (2.5 V), thus activating port 3, while a Gaussian pulse with a suitable frequency spectrum has been input at port 1. Fig. 3 shows the isolation coefficient computed at inactive output port ($S_{21}$) and the transmission coefficients computed at the active one ($S_{31}$). Such results are compared with predictions obtained from linear, frequency-domain simulations performed with the commercial package HP-MDS, showing a satisfactory agreement. Slight discrepancies in Fig. 3 do not depend on the diode model: for MDS simulation, in fact, S-parameters of p-i-n diodes have been described by means of look-up tables, extracted from the same numerical model adopted by LE-FDTD. Differences can hence be ascribed to the different approaches followed to describe wave propagation: in particular, the more comprehensive picture provided by FDTD should allow for a better description of mutual coupling and radiative interactions, which can be considered by MDS only to an approximate extent. The example thus makes the peculiarities of the method described above evident; the proposed extension of the LE-FDTD algorithm allows for physics-based simulation of semiconductor lumped devices, embedded within a full-wave Maxwell solver. It inherently takes into account fabrication process details, as well as propagation issues (such as cross-talk and dispersion), which are hard to describe with more conventional approaches. It therefore provides a useful mean for technology optimization of high-speed integrated circuits.

## REFERENCES

[1] K. S. Yee, "Numerical solution of initial boundary value problems involving Maxwell's equation in isotropic media," *IEEE Trans. Antennas Propagat.*, vol. 14, pp. 302–307, 1966.

[2] A. Taflove, *Computational Electrodynamics*. Norwood, MA: Artech House, 1995.

[3] W. Sui, D. Christensen, and C. Durney, "Extending the two-dimensional FD-TD method to hybrid electromagnetic systems with active and passive lumped elements," *IEEE Trans. Microwave Theory Tech.*, vol. 40, pp. 724–730, 1992.

[4] V. Thomas, M. Jones, and R. Mason, "Coupling of the PISCES device modeler to a 3-D Maxwell FDTD solver," *IEEE Trans. Microwave Theory Tech.*, vol. 43, pp. 2170–2172, 1995.

[5] P. Ciampolini, P. Mezzanotte, L. Roselli, D. Sereni, R. Sorrentino, and P. Torti, "Simulation of HF circuits with FDTD technique including nonideal lumped elements," in *IEEE Int. Microwave Symp.*, Orlando, FL, May 1995, pp. 361–364.

[6] D. Scharfetter and H. Gummel, "Large-signal analysis of a silicon READ diode oscillator," *IEEE Trans. Electron Devices*, vol. 26, pp. 64–77, 1969.

[7] G. Baccarani, M. Rudan, R. Guerrieri, and P. Ciampolini, "Physical models for numerical device simulation," in *Process and Device Modeling*. Amsterdam, The Netherlands, 1986.

[8] J. F. Luy, K. M. Strohm, and E. Sasse, "Si/SiGe MMIC technology," in *IEEE Int. Microwave Symp.*, vol. 3, San Diego, CA, May 1994, pp. 1755–1757.

[9] R. H. Caverly and G. Hiller, "The frequency-dependent impedance of p-i-n diodes," *IEEE Trans. Microwave Theory Tech.*, vol. 37, no. 4, pp. 787–790, 1989.

[10] Z. Abid and A. Gopinath, "Impedance and switching of GaAs p-i-n diodes," *IEEE Trans. Microwave Theory Tech.*, vol. 38, pp. 1526–1528, 1990.

[11] G. Mur, "Absorbing boundary conditions for the finite-difference approximation of the time-domain electromagnetic-field equations," *IEEE Trans. Electromagn. Compat.*, vol. EMC-23, no. 4, pp. 377–382, 1981.